Fatigue Behaviour of Ultrafine Grained Light Alloys

Yuri Estrin[1,a] and Alexei Vinogradov[2,b]

[1] ARC Centre for Design in Light Metals, Department of Materials Engineering, Monash University, and CSIRO Division of Materials Science and Engineering, Clayton, Victoria, Australia

[2] Department of Intelligent Materials Engineering, Osaka City University, Osaka 558-8585 Japan

[a]yuri.estrin@eng.monash.edu.au, [b]alexei@imat.eng.osaka-cu.ac.jp

Keywords: light alloys, fatigue, ultrafine grain, severe plastic deformation, crack growth

Abstract. In this talk we give an overview of the available data on the response to cyclic loading of light alloys whose grain structure has been reduced to the micron or submicron scale by severe plastic deformation (SPD). While the enhancement of tensile strength by this extreme grain refinement can be quite appreciable, the fatigue strength usually does not follow suit. This observation is common to Al, Mg and Ti based alloys and does not appear to be attributable to a particular crystallographic structure. The paper tries to analyse the various effects that may influence this behaviour and identifies the alloying effects as the main contributors to fatigue strength. Their direct impact on fatigue strength is usually stronger than the indirect one, which enters through the composition effect on the grain refinement. Examples from literature and the authors' own research are presented to support the views expressed in the paper.

Introduction

Grain size can be regarded as a key structural factor affecting nearly all aspects of the mechanical behaviour of metals, including fatigue behaviour. Hence, control over the grain size has long been recognised as an avenue for designing materials with desired properties. Most physical and mechanical properties of materials benefit greatly from grain size reduction. Among the procedures devised for grain refinement, severe plastic deformation (SPD) techniques [1], which emerged in the past two decades, are of particular interest. These techniques enjoy great popularity owing to their ability to produce considerable grain refinement down to sub-micron grain size range in bulk-scale work pieces, thus giving promise for structural applications. Nowadays many variants of SPD techniques are readily available. These include equal channel angular pressing (ECAP), accumulative roll bonding (ARB), multistep forging (MF), continuous confined strip shearing (C2S2), etc., having good scaling-up capabilities needed to meet industrial standards. Ultrafine grained (UFG) metals produced by SPD exhibit a promising combination of mechanical properties under monotonic loading. Particularly, for light alloys with the UFG structure, a high specific strength is often coupled with relatively high ductility, which is in many cases found to be higher than for conventionally cold worked materials with relatively coarse grain (CG) size.

However, conflicting results were reported: while some authors claimed increased tensile ductility (in terms of elongation to failure), others observed a reduced ductility of UFG materials compared to the CG ones. In evaluating the results obtained by different authors, one should bear in mind a broad diversity of structural states and processing schedules used in SPD, cf. Table 1 were the results relevant to the present review are compiled. Usually, when comparing ultrafine-grained SPD-manufactured materials with the fully annealed coarse grained ones, a tremendous enhancement of strength and concomitant loss of ductility upon SPD processing is observed. However, in some cases the ductility of SPD-treated materials may be higher than that of their conventionally strain hardened analogues. Thus, enhancement of ductility has been convincingly demonstrated for ECAP-processed commercial purity Al, as well as ARB-processed UFG Al and AA6016 [2-4]. No improvement of ductility was found in non age-hardenable Al-Mg alloys, such as AA5056 [5,6]. On

the other hand, the age-hardenable Al-alloys were found to be most responsive to SPD in terms of structure refinement, strength enhancement and fatigue life and ductility improvement [7-12]. For example, Roven et al. [12] reported a considerable (25-35%) increase in the ultimate tensile strength, σ_{UTS}, in various Al alloys of the 6xxx series in comparison with their conventional T6-heat treated analogues. Not only was this strength increase achieved without compromising ductility, but, in fact, tensile elongation to rupture even *increased* by a factor of 1.5 to 2. The most impressive ductility enhancement was observed for Mg alloys subjected to ECAP [13-15], which is supposed to be due to specific textures forming by simple shear in h.c.p. materials. Record tensile elongations were reached in ECAP processed Mg alloys ZK60 [14, 16] and AZ31 [17] in the superplastic deformation regime. An exceptionally good combination of tensile strength and ductility was also achieved with titanium processed by ECAP [18].

It should be noted that a simplistic approach utilising the Hall-Petch relation, in which enhancement of strength is expected to be achievable by mere grain refinement induced by ECAP processing, does not necessarily work with h.c.p. Mg or Ti based alloys. Indeed, the texture produced in these alloys by ECAP with the commonly used 90º angle between the entrance and the exit channels leads to the predominant orientation of the basal planes at 45º to the pressing direction [19-21]. Basal slip is thus relatively easily activated in subsequent tensile tests for tensile direction aligned with or close to the pressing direction. The texture-related reduction in the yield strength acts against the strength enhancement due to grain refinement, while ductility is improved, as was demonstrated for Mg alloy AZ31 [13].

For prospective engineering applications, the fatigue properties are often of primary importance. These properties have being extensively studied in relation to light alloys, but to our knowledge, no systematic evaluation of the many results available in the literature was conducted to date. So far, most of the experimental results related to fatigue of UFG light alloys were obtained on specimens produced by ECAP in combination with other thermo-mechanical treatments. This paper aims at reviewing and summarising the fatigue data on UFG light alloys processed primarily by ECAP.

The following issues will be addressed in the present review:

1) Effect of impurities on strengthening and fatigue behaviour.
2) Low-cycle fatigue (LCF) and the significance of cyclic softening (or lack thereof).
3) High cycle fatigue (HCF), with the emphasis on the endurance limit.
4) Crack growth resistance.

Approach towards fatigue life improvement

Figure 1 illustrates a traditional fatigue improvement strategy based on the following tenet: *the higher the strength under monotonic loading, the higher is the endurance (fatigue) limit*. Of course, there exist many variations and deviations from this 'rule', and the strategy of improving fatigue properties by raising the ultimate strength can be effective to various degrees depending on the material. Despite considerable grain size reduction and improvement of the materials' performance under monotonic loading by SPD, the high-cycle fatigue properties in general and the endurance limit in particular remain below the expectations for many light alloys. For example, the fatigue results for AA5056 [5,6] and some Al-Mg-Sc [9,10] alloys may look somewhat discouraging when compared with those for conventionally treated samples.

In general, most fatigue tests of nanostructured or ultrafine grained light alloys produced by SPD techniques demonstrate the same trend: their high cycle fatigue (HCF) strength is considerably higher

than that of their coarse grain counterparts. Unfortunately, this effect is not as pronounced as the improvement of strength under monotonic loading. Indeed, while for conventional metals the ratio of the endurance limit to the ultimate tensile strength is typically greater than 0.5, the 'ceiling' value of 0.5 has commonly not been exceeded for UFG alloys, as clearly seen in Fig. 1, where the regression line through the data points has a smaller slope. More alarming is the fact that for the low cycle fatigue regime the results are even worse: UFG and nanostructured metals and alloys are consistently inferior in their ability to sustain cyclic loads – regardless of the SPD technique by which they have been processed. The inferior LCF performance of ultrafine grained and nanocrystalline metals can be rationalised in terms of greater availability of grain boundaries in orientations favourable for crack propagation in a material with the UFG structure.

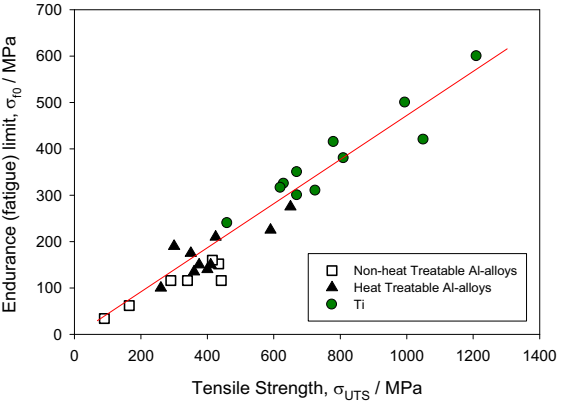

Figure 1. Proportionality between the tensile strength and the endurance limit for light alloys (data from Table 1)

The most successful example of the use of this strategy in combination with SPD techniques was demonstrated by the group of R.Z. Valiev for Ti [22-26]. They started by ordinary ECAP processing of commercially pure Ti and then designed more and more sophisticated strain hardening schedules involving cold rolling, forging and/or drawing to 'convert' the residual ductility after ECAP into strength. This strategy can be most simply illustrated in terms of the total strain approach to the fatigue life assessment.

The LCF and HCF regimes are conventionally distinguished on the basis of the applied strain amplitude [4,27]. HCF testing corresponds to probing a material's resistance to crack initiation, whereas LCF testing corresponds to assessing the material's defect tolerance in a regime when fatigue life is controlled by crack propagation. Combining these two regimes, it is convenient to consider the total strain range $\Delta\varepsilon_t$ as consisting of two additive components – the elastic, $\Delta\varepsilon_{el}$, and the plastic, $\Delta\varepsilon_{pl}$, ones: $\Delta\varepsilon_t = \Delta\varepsilon_{el} + \Delta\varepsilon_{pl}$. An empirical formula relates the total fatigue life (the number of cycles to failure, N_f) to $\Delta\varepsilon_t$ as follows:

$$\frac{\Delta\varepsilon_t}{2} = \frac{\sigma_f'}{E}(2N_f)^b + \varepsilon_f'(2N_f)^c, \qquad (1)$$

where the first and the second terms on the right-hand side correspond to the elastic and the plastic components of the total strain, respectively; E is the Young's modulus, σ_f' is the fatigue strength (which is supposed to be related to the yield stress or the ultimate tensile strength of the material), b is the Basquin exponent, ε_f' is the fatigue ductility coefficient and c is the fatigue ductility, or the Coffin-Manson exponent. Hence, the fatigue life under a given total strain amplitude is expressed in terms of four materials parameters: ε_f', σ_f', c and b; (obviously, both exponents, b and c, are negative.) Although direct equivalence of the parameters ε_f' and σ_f' to the tensile ductility and the ultimate tensile strength, σ_{UTS}, respectively, is rarely observed in experiment, a correlation between

these pairs of quantities does exist pretty often. At high strain amplitudes corresponding to short fatigue lives, the plastic strain component is prevalent in the total applied strain and the fatigue life is determined primarily by ductility. At long fatigue lives, the elastic strain amplitude is more significant than the plastic one, and fatigue life is dictated by the fracture strength, so that the endurance limit increases with tensile strength [25], Fig. 1. As mentioned above, the unfortunate reality is that in most cases the highest strength levels are achieved at the expense of ductility, cf. Table 1. Process design targeting enhancement of fatigue properties is hindered by the fact that no commonly accepted physically based models capable of explaining the physical origin and predicting the values of the four parameters $\varepsilon_f^{'}, \sigma_f^{'}$, c and b, which enter Eq.(1), are available to date even for structurally simple pure polycrystals.

Cyclic response of UFG light alloys

In low cyclic fatigue testing under constant total or plastic strain amplitude, the cyclic response exhibits remarkable variations in the stress amplitude depending on the type of slip and purity of the material. Beside the different stress amplitude levels, a distinctly different cyclic hardening/softening behaviour is observed for the various alloys, Fig. 2. It has long been recognised that the microstructure of high purity metals produced by SPD is inherently unstable and is prone to recovery and grain coarsening at low homologous temperatures, e.g. at room temperature, even in the absence of loading [28,29]. Under cyclic deformation, softening (i.e. a decrease of stress amplitude with the number of cycles or the cumulative strain for a given strain amplitude) is often observed for relatively pure single-phase f.c.c. UFG materials such as pure Al or Cu, see [4] and references therein. Cyclic softening in pure metals is usually associated with the ease of dislocation annihilation and is inherited from plastic pre-staining regardless of how severe it was. In this sense cyclic softening underscores the similarity in the behaviour of ultrafine grained and conventional cold worked materials, rather than drawing a boundary between them. A mechanism of cyclic softening associated with dynamic grain coarsening, which is specific to SPD processed metals suggested by Mughrabi and Höppel [30] is illustrated in Fig. 3b where the coarsened grains aligned with two intersecting shear bands are visible on the SEM electron channeling contrast (ECC) image of fatigued UFG commercial purity Al. The rate of softening depends strongly on the initial structure and loading conditions and may vary in a wide range. Furthermore, the rate of grain coarsening depends strongly on the grain boundary mobility, which is controlled to a large extent by the impurity content. Therefore, by restricting dislocation and grain boundary mobility through alloying it is possible to alleviate or completely eliminate cyclic softening, as can be seen for Al alloys, Fig. 2.

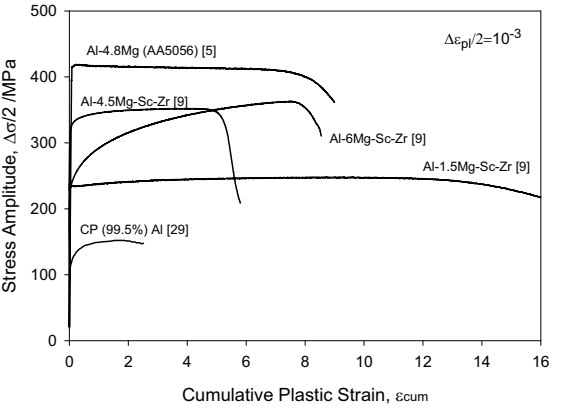

Figure 2. Cyclic response of ECAP processed Al and various Al-Mg alloys under the same constant plastic strain amplitude; note (i) different stress levels increasing with the content of the alloying elements and (ii) different cyclic softening/hardening behaviour

It was shown that grain coarsening, often associated with macroscopic shear banding in cyclically deformed SPD metals, Fig.3a, depends on the plastic strain amplitude, time (strain rate) and temperature [30-33], but it is most strongly dependent on the purity of the material. In commercial purity 99.5% UFG Al with a grain size of 350 nm [31,32], the low purity results in a reduced dynamic grain coarsening and appreciable cyclic hardening. Aluminium alloys, e.g. a single-phase Al-Mg alloy AA5056, show some slight cyclic softening under much higher stress amplitudes than those observed for commercial purity (CP) Al. As grain (dislocation cell) coarsening in this AA5056 alloy is not pronounced, cyclic softening is attributed primarily to the dislocation recovery. In the precipitation hardenable Al-Mg-Sc alloys, the numerous precipitates stabilise the structure decisively, so that it remains ultrafine- or fine-grained during annealing for 1 h at temperatures up to 400^{o}C. No grain coarsening was observed after low- or high-cycle fatigue of this alloy [9,10]. Increasing amount of Mg results in greater tensile strength and higher level of cyclic stress amplitude, while increasing processing temperature (cf. Al-6Mg-Sc curve, Fig. 2) leads to formation of fine (10 μm), rather than ultrafine, grain structure exhibiting considerable cyclic hardening due to ordinary dislocation accumulation. As distinct from the above results on the stabilising effect of precipitation hardening, Liu and Wang [34] reported a rapid cyclic softening in ECAP processed 8090 Al-Li alloy that was age hardened and contained fine coherent precipitates. The observed softening can possibly be associated with dislocation cutting through the shearable precipitates, leading to partial dissolution and/or disordering of precipitates during fatigue, similar to what was observed in ECAP processed Cu-Cr-Zr alloy [35]. Coarse Al_3Sc particles dispersed in Al-Mg-Sc alloys are extremely stable and cannot be sheared by gliding lattice dislocations and, thus, no cyclic softening is observed. Ultrafine grained hcp metals, such as ECAP processed titanium, were found to be immune from any cyclic softening and macroscopic shear banding [23] despite very high stress amplitudes in these metals under plastic strain control.

Higher stress levels, lower ductility and susceptibility to strain localisation in macroscopic shear bands in UFG Al and Al-alloys, Fig. 3, result in reduced LCF life as compared to those of fully annealed reference alloys [4]. Nevertheless, the LCF properties can be considerably improved by post-ECAP annealing at moderate temperatures, which reduces the initial dislocation density, the internal stresses and the number of stress risers and also leads to relaxation of stressed grain boundaries. In particular, it was suggested that by producing a bi-modal grain structures with co-existing populations of small and large grains a favourable combination of strength and ductility may be achieved, which also promotes improved fatigue performance. This can, indeed, apply to LCF due to higher ductility associated with the presence of coarse grains, but has not been confirmed for HCF [36]. Indeed, coarse grains yield at lower stresses than the rest of the polycrystal, thereby providing a natural pathway for early strain localisation and premature failure either due to cracking at the interfaces between the coarse grains and the surrounding fine-grain matrix or due to transgranular surface crack initiation in a coarse shear band.

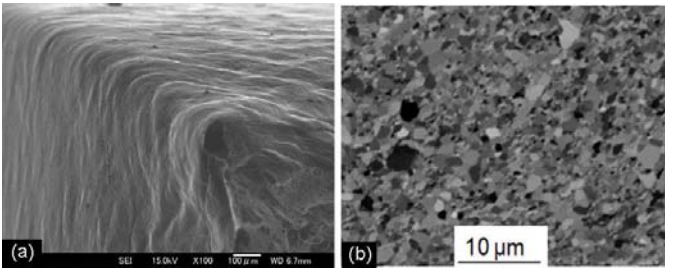

Figure 3. SEM micrograph showing typical shear band morphology on the side surface of fatigued UFG ECAP Al-Mg alloy AA5056 (a) and ECC image of the intersecting shear bands with coarsened grains in cyclically deformed CP Al (b)[30](Courtesy H. Mughrabi and H.W. Höppel)

The enhancement of ductility of SPD-treated Mg alloys, Table 1, is a factor favouring betterment of their LCF properties. Wu et al. [15] have demonstrated for the AZ31B alloy that the LCF life resulting from combining effects of grain refinement and texture, can be enhanced through ECAP up to two passes, but further pressing to 8 passes results in a decrease of fatigue life. A similar conclusion was drawn by Chung et al. [7] regarding the HCF live of ECAP processed AA6061 alloy. These results are akin to those reported for AA5056 alloy subjected to ECAP [5,6]. Like for Al alloys, the endurance limit of hot-rolled Mg alloy AZ31 was not improved by ECAP (4 passes, Route Bc) either - despite considerable grain refinement and the associated Hall-Petch strengthening [13], cf. [37]. This similarity of HCF behaviour after ECAP processing for these different material groups may reflect a general regularity, but may also be fortuitous. The role of interplay between strength and ductility influenced by ECAP processing (both being affected by ECAP-induced texture) is yet to be understood.

High-cycle fatigue resistance

In line with the results by Roven et al. [12] and Gubicza et al. [38] on strength under monotonic loading, one can see, Fig. 2, that the cyclic response at low and high strains depends strongly on the composition, e.g. Mg and Sc content in Al alloys: the higher the degree of alloying, the stronger is the response in terms of stress amplitude for a given strain amplitude. This is true for both non-heat treatable solid solutions and precipitation strengthened heat-treatable alloys. The same trend is seen in high-cycle regime, Fig. 4a: icreasing Mg content in Al-alloys results in longer fatigue life for the same stress amplitude [5,39]. In particular, in Al-Mg-Sc alloys the considerably enhanced HCF properties were demonstrated for a commercial alloy 1570 (Russian designation) [40], Fig.4b, and for an AA6106 Al-Mg alloy with additions of Zr and Sc [11]. Compared to the rather modest results of Vinogradov et al. [9,10] for various ECAP processed Al-Mg-Sc model compositions (cf. [41,42]), the successful results reported in Refs. [40] should be attributed to a higher content of Sc and a combination of Sc with Zr [11], leading to a larger volume fraction of strengthening particles after optimised aging, rather than to the features of SPD processing.

Obviously, cyclic plastic deformation plays a key role in all aspects of fatigue. It determines the cyclic response of materials at all strain amplitudes, i.e. in the HCF range where fatigue life is controlled by crack nucleation in a smooth body and in the LCF regime corresponding to crack propagation. The intrinsic micromechanisms responsible for the cyclic response differ for different materials, depending on the primary strengthening mechanisms. In UFG pure materials the resistance to cyclic deformation has two components: (i) dislocation-dislocation interaction and (ii) dislocation-grain boundary interaction. In solid solutions, the dislocation-impurity interaction has to be added to the above two, while in the precipitation hardened materials the interaction of dislocations with the second-phase particles is essential, and, moreover, it may play a key role in the stability and overall fatigue performance of age-hardenable alloys.

The effect of the ECAP-induced grain refinement on the fatigue properties of commercial purity (CP) titanium is illustrated in Fig. 5, where application of the strengthening strategy by structure refinement, strain hardening and impurity hardening is most rationally utilized for improvement of fatigue. This is one of a few examples where both the HCF and the LCF properties are improved with the reduction of the grain size d by ECAP. (At least the LCF fatigue resistance did not degrade after 8 ECAP pressings using Route B_c) [23] if compared to those in coarse grain counterparts [45].

In fact, the fatigue limit of CP Ti reached or even exceeded that of conventionally manufactured Ti alloys, which makes UFG Ti extremely attractive for biomedical applications as a substitute for less bio-compatible Ti alloys in implant surgery. It is worth mentioning that the significant improvement of HCF properties is achieved already after the first ECAP passes [48]. The results for Al alloys [7] and Cu [36] pressed to a small number of passes (1 or 2) suggest that processing to moderate, rather than excessively high, strains may offer an attractive trade-off between the processing cost and

energy efficiency and improvement of fatigue properties, particularly if HCF is of primary concern. The judicious choice of processing parameters, such as temperature, strain rate and back pressure, and the initial state of the material becomes decisive for ensuring the ultimate performance after reasonably moderate straining.

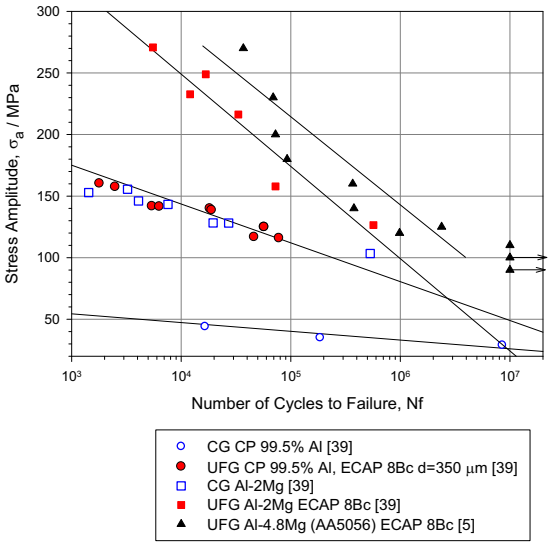

(a)

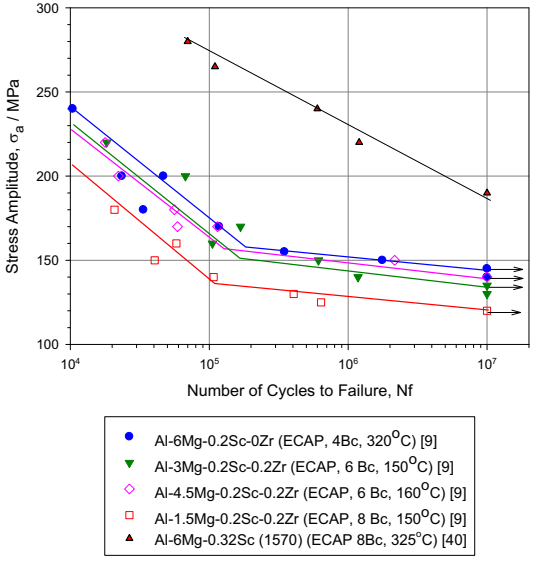

(b)

Figure 4. High-cycle fatigue properties of (a) commercial purity Al and Al-Mg solid solutions and (b) age-hardened Al-Mg-Sc alloys; arrows represent run-out tests

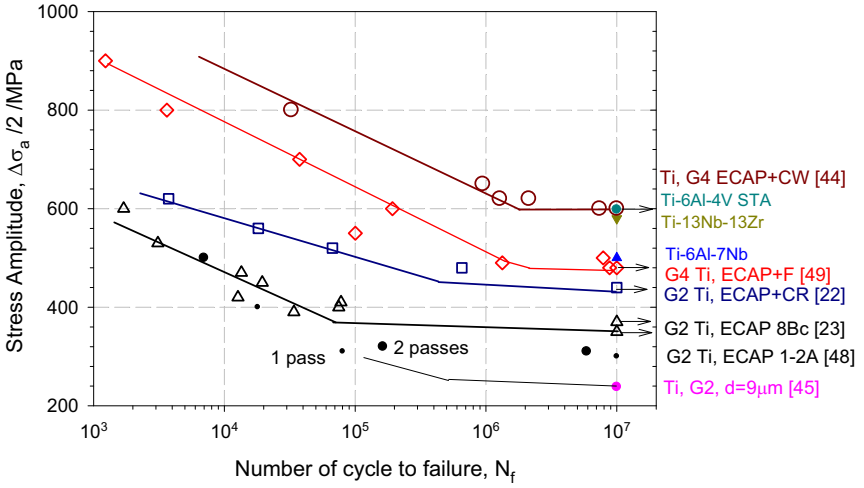

Figure 5. Fatigue curves for CP Titanium with different grain size obtained by ECAP processing; all abbreviations are explained in the caption to Table 1

Crack growth behaviour

The LCF life assessment of smooth bodies delivers only indirect information regarding the resistance to flaws - either pre-existing or formed in the course of cycling. Comprehensive understanding of fatigue properties requires evaluation of the fatigue crack growth, which has been only scarcely studied to date. The crack growth resistance tests on the non-heat treatable ECAP 5056 Al-4.8Mg alloy using the compact tension (CT) specimens were performed in Ref. [6]. Figure 6 shows the crack growth rate *da/dN* in light metals and alloys manufactured by ECAP as a function of the stress intensity factor range $\Delta K=K_{max}-K_{min}$ given by

$$\Delta K = Y\Delta\sigma\sqrt{\pi a} \ . \tag{2}$$

(In the above expressions Y is a numerical factor dependent upon the specimen/crack geometry, $\Delta\sigma=\sigma_{max}-\sigma_{min}$ is the applied stress range, a is the crack length, and N is the cycle number) for a given stress ratio $R=\sigma_{min}/\sigma_{max}=0.1$. The *da/dN* vs. ΔK plots for UFG materials exhibit the same stages of crack propagation as those well-known for conventional polycrystals, i.e. (1) slow crack advance in the near 'threshold' region, (2) an intermediate stage and (3) unstable crack growth at high ΔK values. In stage 2 crack propagation, the Paris law applies:

$$\frac{da}{dN} = C\left(\Delta K\right)^m , \tag{3}$$

where C and m are material parameters. It was found that the fatigue 'threshold' ΔK_{th} corresponding to the low-end limit of the curve decreased after ECAP of a non-heat treatable AA5056 Al-Mg alloy [6], as shown in Fig. 4a. Very similar results were obtained by Hübner et al [50] for CP Al, Chung et al. [7] for the heat treatable UFG AA6061 Al alloy and by Kiessling et al. [51] and Hanlon et al. [52] for Ti. It was shown that in all cases the crack growth rate in the near-threshold region is higher in the UFG state than in the ordinary polycrystalline reference materials; however, the picture might be opposite for relatively high stress intensity factor ranges ΔK. Compared to conventional materials

with larger grains, fatigue cracks in the UFG specimens propagated with much less out-of-plane deflections, Fig.7, providing faster fatigue crack growth rates under limited crack tip plasticity. The latter is known to be the most effective mechanism of crack tip blunting. Grain refinement and strain hardening limiting the dislocation mobility inevitably result in suppression of this favourable crack tip blunting effect, thus leading to faster propagation of sharp cracks. Prevalence of the intergranular fracture mode during fatigue crack growth in UFG metals and alloys was observed experimentally. This explained the nearly straight crack path in a uniform equiaxed UFG structure and was assumed to be related to grain boundary weakening by trapped lattice dislocations [53]. A non-uniform, e.g. bi-modal, structure or a structure with a pronounced crystallographic texture may give rise to a more tortuous crack path and enhance the resistance to crack growth, but this issue has yet to be addressed in future studies.

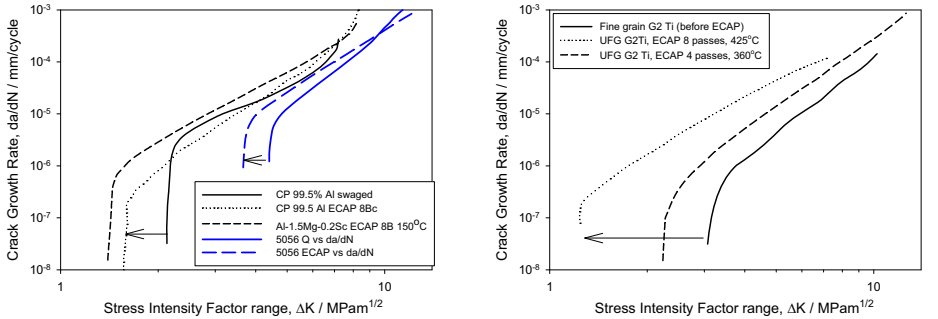

(a) **(b)**

Figure 6. Fatigue crack growth rate as a function of the stress intensity factor range ΔK: (a) in Al and Al-alloys and (b) Grade 2 Ti (b); data compiled from Refs. [6,50, 51] (a) and Refs. [51,52] (b)

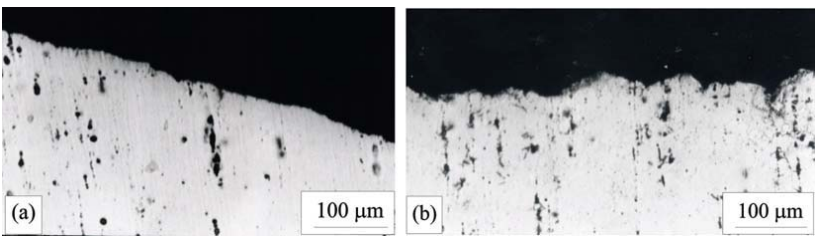

Figure 7. Typical view of fatigue fracture in: (a) UFG and (b) conventional CG AA5056: a nearly straight path with sharp edges is seen in a UFG sample (a), while a tortuous crack path with many deflections is observed in a coarse grain sample (b) (after [6])

In the fracture mechanics approach to fatigue failure, the transition from the near-threshold slow crack growth regime to the intermediate fatigue stage is considered to be accompanied with a transition in the crack behaviour from being strongly microstructure sensitive to becoming microstructure insensitive. Such a transition is often observed when the size r_{cp} of the plastic zone at the cyclic crack tip, which is estimated as

$$r_{cp} = \lambda \left(\frac{\Delta K}{2\sigma_y^{'}} \right)^2 , \qquad (4)$$

becomes comparable with the grain size d [27]. Here λ is a numerical factor of the order of $1/\pi$ and $\sigma_y^{'}$ is the cyclic yield stress determined from the cyclic stress-strain curve. If the stress intensity factor range corresponding to the transition point is denoted as ΔK_T, the last condition provides a transition criterion $r_{cp} = r_{cp}(\Delta K_T) \cong d$. However, estimations of r_{cp} at the transition point yield values which are significantly greater than the average grain size d of the Al alloys tested (e.g. AA5056, AA6161 and Al-1.5Mg-Sc). For example, taking for the Al-Mg alloy AA5056 $\sigma_y^{'}$=280 MPa and for the threshold $\Delta K=\Delta K_{th}$=4.3 MPa·m$^{1/2}$ one obtains r_{cp}=7-8 μm, which is much greater than d=0.3-0.4 μm. This suggests that a large number of neighboring grains may be involved in crack tip plasticity, even near the threshold. Equation (4) at the transition point can be simply generalised as

$$\Delta K_T \cong \sigma_y^{'}\sqrt{d^*} \tag{5}$$

with d^* denoting the characteristic size of a '*structural unit*' within the material responsible for fracture (grain size, sub-grain or cell size, particle size, etc.). It can thus be expected that ΔK_T increases with d^*, which is, indeed, observed in UFG metals as well. Assuming the threshold value ΔK_{th} is approximately equal to ΔK_T, the last relation can be re-written – as is often done in literature - in a more general form

$$\Delta K_{th} = A + B\sqrt{d^*}\,, \tag{6}$$

where A and B are material constants. B is often assumed to be nearly equal to the endurance limit σ_{fo} (conventionally defined as the stress amplitude at 10^7 cycles), so that (dropping A) the last expression can be presented in the form $\Delta K_{th} \cong \sigma_{fo}\sqrt{\pi d^*}$. Observations reported in [6,7,50-53] show that ΔK_{th} in UFG metals processed by SPD is reduced, which qualitatively agrees with Eqs. (5) and (6). The fracture surface analysis of UFG metals [5,6] reveals striations characterising the fatigue crack advance during the stable crack growth stage similar to that in conventional materials. Overall, there is ample similarity between ultrafine grained and conventional polycrystals in their fatigue crack growth behaviour. However, a quantitative microstructurally based explanation of the detrimental effect of grain refinement on fatigue threshold, i.e. its reduction upon ECAP processing, is not straightforward. In this low end regime, fatigue crack growth is strongly influenced by microstructural features, such as the type of dislocation slip, grain dimensions and the characteristics of second phase particles, including their average size and spatial distribution [54]. Often it is very difficult to separate these effects. The fatigue crack growth resistance of age hardened aluminum with fine coherent strengthening particles (e.g. under-aged alloys) is commonly found to be superior, while it is inferior when the particles are coarse and incoherent (e.g. in over-aged alloys) [54]. This was shown to be directly related to tortuosity of the crack path in the material, which is greater in the case of coherent particles, when planar slip on crystallographic slip planes, with multiple deflections at grain boundaries prevails. The fatigue parameters, such as the threshold ΔK_{th} and the maximum stress intensity K_{max}, were also linked to particle spacing playing the role of a "structural unit" length entering Eq. (6) or a more general relation $K_{\max} = \alpha d^{*\beta}$, where α and β are material parameters. Particles with a larger spacing and a lower volume fraction lead to increased out-of-plane cracking and, thus, larger ΔK_{th} and K_{max} [54]. Planarity of slip can be enhanced by alloying through a reduction in the stacking fault energy (SFE) and in the probability of dislocation cross-slip. This has a pronounced effect on ΔK_{th} compared to the case of high SFE when cross-slip promotes the formation of three-dimensional dislocation cell or subgrain structure. This effect is seen in Fig. 6a where the results for pure Al (homogeneous wavy slip) and an Al-Mg alloy AA5056 (planar slip) are compared. Higher SFE values promoting planar slip in the alloy are responsible for the observed higher fatigue threshold values.

At the current level of our understanding of the mechanisms of fatigue in UFG light alloys, it is not possible to make a clear-cut connection between the parameters characterising the crack growth

(e.g. Fig. 6) and the fatigue life curves of the kind shown in Figs. 3-5. In fact, a link between the parameters characterising the crack growth in the Paris law region and the plastic strain related part of Eq. (1) (second term on the right-hand side), particularly between the exponents *b* and *m*, can be made in a straightforward manner. However, it is not possible so far to relate the phenomenological parameters of the fatigue equation to the characteristics of the low end, near-threshold part of the curves in Fig. 6.

Summary and Conclusions

Based on the analysis of experimental data for high- and low-cycle fatigue as well as fatigue crack growth in SPD manufactured metals and alloys belonging to the different material classes (pure, solid solution strengthened and particle strengthened light metals) the following conclusions can be drawn.

Extreme grain refinement by severe plastic deformation generally improves the fatigue performance of Al-, Mg- and Ti-based light alloys. However, the full potential of achieving favourable combinations of grain refinement and texture has certainly not been explored and exploited. A better understanding of the specific mechanisms underlying the response of these materials to cyclic loading may lead to microstructures and textures optimised with respect to the fatigue performance. It should be recognised that complex interplay of the effects of grain refinement, texture and alloy composition makes it extremely difficult to assess the role of the individual effects in the overall change of the fatigue behaviour after SPD (particularly ECAP) processing. The chemical composition appears to plays a key role in the fatigue properties of light alloys. The cumulative effect of solution strengthening and precipitation strengthening may supersede the effect of grain refinement in the overall mechanical response under monotonic and cyclic loading conditions. Thus, we believe that the role of SPD should not be exaggerated: enhanced fatigue properties which have been achieved in specific alloys by SPD processing may well be achievable for alloys with different chemical composition more economically by appropriate conventional thermomechanical treatment. On the basis of the limited data available, it can be anticipated that complex light alloy systems will be most responsive to improvement of fatigue performance by SPD processing. This will be achieved through improvement of the as-cast structure, rearrangement of secondary phases and alteration of precipitation kinetics by producing a finer and more uniform distribution of strengthening particles. The main message of the survey is that it can only be by understanding the role of the individual effects associated with the SPD-induced microstructure and texture that the full potential for improving fatigue performance of light alloys can be taken advantage of.

Acknowledgements

The authors are indebted to Prof. S. Hashimoto, Prof. R.Z. Valiev, Dr. V.I. Kopylov, Dr. R. Lapovok and Dr. T. Lowe for useful discussions and the permission to use their data in this review.

Table 1. Mechanical properties of UFG light alloys produced by SPD

Material			Processing	$\sigma_{0.2}$, MPa	σ_{UTS}, MPa	δ	σ_{fo}, MPa
	AZ31	[13]	SC	50	170	10	40
			HR 370 °C	175	277	21	95
			HR+ECAP 4Bc 200°C	115	251	27	95
		[37]	ST420°C 2h+Q, ECAP4Bc 320-200°C	180	286	9.4	40*
Non-heat treatable	1050 (99.5, CP Al) [M]	[39]	O	28	70	40	28
		[39]	ECAP 8Bc	N/A	N/A	N/A	52
	Al-Mg2†††	[39]	O	N/A	N/A	N/A	100
		[39]	ECAP 8Bc	N/A	N/A	N/A	125
	AA 5056 Al-4.8Mg alloy		O	122	290	43	116
			H18	407	434	10	152
		[5]	ECAP 4C, 150°C	280	340	25	116
		[5]	ECAP 8Bc, 110°C	392	442	7	116
Heat treatable	AA6061 Al alloy		O	150	270	48	40**
			T6	276	310	12	50**
			T6				97
		[7]	ST ECAP, 1, 125°C	310	375	20	80**
		[7]	ST ECAP, 4Bc , 125°C	380	425	20	<60**
	2124		T851	455	492	7.2	125†
		[8]	T851+ECAE 8Bc, BP	330	602	7.2	290††
	Al-4Mg-0.3Sc	[41]	Hot Drawing	315	415	17	160
	Al-5.2Mg-0.32Mn-0.25Sc	[42]	Hot rolled	240	375	29	150
	Al-1.5Mg-0.2Sc-Zr	[9]	ST+ECAP, 8Bc, 150 °C	340	360	13	135
	Al-3.0Mg-0.2Sc-Zr	[9]	ST+ECAP, 6Bc, 150 °C	370	400	15	140
	Al-4.5Mg-0.2Sc-Zr	[9]	ST+ECAP, 6Bc, 160 °C	230	410	29	150
	Al-6.0Mg-0.2Sc-Zr	[9]	ST460°C 24h+ECAP, 4Bc, 320°C	240	260	8	100
	Al-5.7Mg-0.32Sc-0.4Mn	[40]	ST520°C 48h+ ECAP, 8C, 325°C	280	300	8	190
	AA6106## +0.1Zr	[11]	ST, Ag190°C 4h	250	350	23	175
			ST+ECAP 4+ Ag190°C 4h	570	590	9	225
	+0.1Zr+0.5Sc	[11]	ST+AG190°C 2h	375	425	16	210
			ST+ECAP 4+ AG190°C 2h	625	650	8	275
` Ti (Grade 2)			CR	380	460	26	240
		[23]	ECAP 8Bc 400°C	640	810	15	380
		[22]	ECAP 8Bc 400°C, CR 87% A300C 1h	970	1050	8	420
		[46]	ECAP 6Bc 420 °C	630	670	32	350
		[47]	ECAP 4A 360°C	610	780	22	415
		[47]	ECAP 4C 360°C	600	630	26	325
		[47]	ECAP 4CA 360°C	580	620	24	316
		[48]	ECAP 1 BP	620	670	11	300
		[49]	ECAP 2A BP	660	725	13	310
Ti (Grade 4)		[49]	ECAP 450-400C 8Bc+F 400-300°C A	860	995	14	500
		[49]	ECAP 8Bc+F 400-300°C +D	1060	1210	2	600
Ti-6Al-4V (Grade 5)			STA, ST 950°C, Ag 540°C	1100	1170	10	700
		[43]	MF	1180	1300	7	700***
		[44]	SPD+A	1270	1370	11	750

d - grain size, $\sigma_{0.2}$ - conventional yield stress, σ_{UTS} – ultimate tensile strength, δ - elongation at break, σ_{fo} – endurance limit (on the basis of 10^7 cycles, and stress ratio R=-1, if not otherwise specified); processing temperature is shown where it differs from ambient, CR – cold rolling, HR – hot rolling, F - forging, D – drawing, MF – multistep forging, ST-solution treatment, Q – quenching, A - annealing, AG – ageing, BP - back pressure; * R=0.05, ** R=0, *** R=0 rotation-bending test 500Hz; † based on $5x10^8$ cycles; †† data obtained from the total strain controlled test at about $2x10^5$ cycles to failure; ††† data obtained from the total strain amplitude controlled test at about 10^6 cycles to failure; ## data for these alloys were estimated from original published graphs.

References

[1] R.Z. Valiev, Y. Estrin, Z. Horita, T.G. Langdon, M.J. Zehetbauer, Y.T. Zhu: JOM 58 (2006) 33.
[2] H.W. Höppel, J. May, P. Eisenlohr, M. Göken, Z. Metallkunde 96 (2005) 566.
[3] H.W. Höppel, J. May, M. Göken: Adv. Eng. Mater. 6 (2004) 781.
[4] H. Mughrabi, H.-W. Höppel and A. Vinogradov: in *Bulk Nanostructured Materials*, M.J. Zehetbauer and Y.T. Zhu eds., WILEY–VCH (2006).
[5] V. Patlan, A. Vinogradov, K. Higashi and K. Kitagawa: Mater. Sci. Eng. A300 (2001) 171.
[6] A.Vinogradov, V. Patlan, K. Kitagawa, M. Kawazoe: Nanostr. Mater. 11 (1999) 925.
[7] C.S. Chung, J.K. Kim, H.K. Kim, W.J. Kim: Mater. Sci. Eng. A337 (2002) 39.
[8] R. Lapovok, C. Loader, F. Dalla Torre and S.L. Semiatin: Mater. Sci. and Eng. A425 (2006) 36.
[9] A. Vinogradov, A. Washikita, K. Kitagawa, V.I. Kopylov: Mater.Sci.Eng. A349 (2003) 318.
[10] A. Washikita, K. Kitagawa, V.I. Kopylov and A. Vinogradov: in Ultrafine Grained Materials II, eds. Y.T. Zhu, T.G. Langdon, R.S. Mishra, S.L. Semiatin, M.J. Saran and T.C. Lowe: TMS, (2002) 341.
[11] P. Cavaliere and M. Cabibbo: Mater. Characterization 59 (2008) 197.
[12] H. J. Roven, H. Nesboe, J. C. Werenskiold and T. Seibert: Mater. Sci. Eng. A410-411 (2005) 426.
[13] Z. Zuberova, L. Kunz, T.T. Lamark, Y. Estrin, M. Janecek: Metall. and Mater. Trans. A 38 (2007) 1934.
[14] R. Lapovok, P.F. Thomson, R. Cottam and Y. Estrin: Mater. Trans. 45 (2004) 2192.
[15] L. Wu, G.M. Stoica, H.H. Liao, S.R. Agnew, E.A. Payzant, G. Wang, D.E. Fielden, L. Chen and P. Liaw: Metal. Mater. Trans. A 38A (2007) 2283.
[16] R. B. Figueiredo, T. G. Langdon: Adv. Eng. Mater. 10 (2008) 2008, 37.
[17] R. Lapovok, Y. Estrin, M. Popov, T.G. Langdon: Adv. Eng. Mater.10 (2008) 429.
[18] R.Z.Valiev, Nature Materials 3 (2004) 511.
[19] T. Mukai, M. Yamanoi, H. Watanabe, K. Hiqashi: Scripta Mater. 45 (2001) 89
[20] S.R. Agnew, J.A. Horton, T.M. Lillo, D.W. Brown: Scripta Mater. 50 (2004) 377.
[21] S.R. Agnew, P. Mehrotra, T.M. Lillo, G.M. Stoica, P.K. Liaw: Acta Mater. 53 (2005) 3135.
[22] V.V. Stolyarov, I.V. Alexandrov, Yu.R. Kolobov, M. Zhu, T. Zhu and T. Lowe: in *Fatigue'99*, ed. by Wu, X.R., Wang, Z.G.; Higher Education Press, P.R.China, (1999) Vol.3, 1345.
[23] A.Vinogradov, V.V. Stolyarov, S. Hashimoto and R.Z. Valiev: Mater. Sci. Eng. A318 (2001) 163.
[24] V.V. Stolyarov, Y.T. Zhu, T.C. Lowe and R.Z. Valiev: Mater. Sci. Eng. A303 (2001) 82.
[25] V.V. Stolyarov, Y.T. Zhu, I.V. Alexandrov, T.C. Lowe and R.Z. Valiev: Mater. Sci. Eng. A343 (2003) 43.
[26] V.V. Stolyarov, Y.T. Zhu, T.C. Lowe and R.Z. Valiev: Mater. Sci. Eng. A299 (2001) 59.
[27] S. Suresh: *Fatigue of Materials*; Cambridge University Press, 1991.
[28] H.Miyamoto, T.Mimaki, A.Vinogradov and S.Hashimoto: Annales de Chimie 27 (2002) S197-S206
[29] W. Skrotzki, N. Scheerbaum, C.-G. Oertel, H.-G. Brokmeier, S. Suwas and L.S. Tóth: Acta Mater. 55 (2007) 2211.
[30] H. Mughrabi and H.W. Höppel: Mat. Res. Soc. Symp. Proc. Vol. 634 (2001) B2.1.1.
[31] H.W. Höppel, C. Xu, M. Kautz, N. Barta-Schreiber, T.G. Langdon, H. Mughrabi, in: *Nanomaterials by Severe Plastic Deformation* (M. Zehetbauer, R.V. Valiev, Eds); Wiley-VCH, Weinheim; 2004; 676.
[32] H.W. Höppel, Z.M. Zhou, H. Mughrabi, R.Z. Valiev: Phil. Mag. A82 (2002) 1781.
[33] H. Mughrabi, H.W. Höppel, M. Kautz: Scripta Mat. 51 (2004) 807.
[34] S.M. Liu and Z.G. Wang: Scripta Mater. 48 (2003) 1421.
[35] A. Vinogradov, T. Ishida, K. Kitagawa, and V.I. Kopylov: Acta Mater. 53 (2005) 2181.
[36] A. Vinogradov and S. Hashimoto: presentation at the TMS Meeting, New Orleans, USA (2008) (unpublished work)
[37] H.-K. Kim, Y.-In Leea, C.-S. Chung, Scripta Materialia 52 (2005) 473.
[38] J. Gubicza, N.Q. Chinh, Z. Horita, T.G. Langdon: Mat. Sci. Eng. 387–389 (2004) 55.
[39] J. May, M. Dinkel, D. Amberger, H.W. Höppel and M. Göken: Mettal. Mater. Trans. A 38A (2007) 1941.
[40] E.V. Avtokratova, R.O. Kaibyshev and O. Sh. Sitdikov: Phyz. Metal. Metallovedenie, 105 (2008) 532.
[41] T. Wirtz, G. Lütejering, A. Gysler, B. Lenczowski and R. Rauh: Mater. Sci. Forum, 331-337 (2000) 1489.
[42] O. Roder, T. Wirtz, A. Gysler and G. Lütejering: Mater. Sci. Eng. A234-236 (1997) 181.
[43] S. Zherebtsov, G. Salishchev, R. Galeyev and K. Maekawa: Mater. Trans., 46 (2005) 2020.
[44] I.P. Semenova, V.V. Latysh, G.I. Raab, R.Z. Valiev and T. Lowe: TMS Annual Meeting, New Orleans, USA (2008) (oral presentation by R.Z. Valiev).
[45] N.G. Turner and W.T. Roberts: Trans. AIME 242 (1968) 1223.

[46] W.-J. Kim, C.-Y. Hyun, H-K. Kim: Scripta Mater. 54 (2006) 1745.
[47] A. Vinogradov, S. Hashimoto and V.I. Kopylov: unpublished work.
[48] R. Lapovok, T. Lowe, A.Vinogradov, S. Hashimoto: unpublished work.
[49] A. Vinogradov, K. Kitai, S. Hashimoto, I. Semenova, R.Z. Valiev, T. Lowe: unpublished work
[50] P. Hübner, R. Kisseling, H. Biermann, T. Hinkel, W. Jungnickel, R. Kawalla, H.W. Höppel and J. May: Metall. Mater. Trans A, 38A (2007) 1926.
[51] R. Kiessling, P. Hübner, H. Biermann and A. Vinogradov: Int. J. of Mater. Research, 97 (2006) 1566.
[52] T. Hanlon, E.D. Tabachnikova and S. Suresh: Int.J. Fatigue 27 (2005) 1147.
[53] A. Vinogradov: J. Mater. Sci., 42 (2006) 1797.
[54] K. Vasudevan, K. Sadananda and K. Rajan: Int. J. of Fatigue, 19 (1997) 151.